COBEM 2023 27TH INTERNATIONAL CONGRESS OF MECHANICAL ENGENEERING

ABCM Brazilian Society of Mechanical Sciences and Engineering
27th ABCM International Congress of Mechanical Engineering
December 04-08, 2023, Florianópolis-SC, Brazil

COB-2023-1490
Study Of The Elastic Behavior Of The Secondary Suspension Spring Set in The Y32 Bogie Utilized in Vale Passenger Car

Victor Hugo Garcia de Campos
Ryan David Earl
Marco Lúcio Bittencourt
School of Mechanical Engineering – University of Campinas – UNICAMP
v164332@dac.unicamp.br; r230367@dac.unicamp.br; mlb@unicamp.br

Leonardo Bartalini Baruffaldi
Federal Institute of São Paulo – IFSP
leonardo.baruffaldi@ifsp.edu.br

Julismar Dadalto Santos
Vale S.A.
C0634896@vale.com

Abstract. *This work details a study about the elastic behavior of a railroad passenger car secondary suspension spring pack equipped on Y32 bogies, which are used on the Vitória to Minas and Carajás railroads. The referred spring pack is composed of a steel coil in parallel with two rubber springs assembled in series, yielding a non-linear stiffness behavior. It is known that the secondary suspension plays an important role on derailment indices and on wheel-rail wear, stressing the importance of reliable and realistic mechanical properties to simulate such phenomena. In this work, we develop a finite element model for the spring pack, using experimental data to calibrate the rubber components. This model is used to estimate the spring stiffness properties and to simulate the vehicle dynamical behavior using multibody dynamics. Results show that the non-linearities have considerable influence on the system response, suggesting that the use of rubber/steel coil springs on secondary suspensions deserve special attention.*

Keywords: *Railway vehicle suspension, non-linear stiffness, Finite Element Method, Rubber Spring, multibody dynamics.*

1. INTRODUCTION

The railroad vehicle suspension plays a fundamental role in passenger safety and comfort. The railway operation is subjected to a plethora of different vibrations that, from the wheel-rail contact side, should be kept under straight amplitude control to prevent derailments, and also excessive wear. On the passengers side, both accelerations and displacements must be controlled to allow for a comfortable ride (Eickhoff *et al.*, 1995). It is essential, therefore, that the mathematical model used for design and simulation of suspensions is as good as possible to assure a realistic assessment of vehicle dynamic responses.

Passenger railroad vehicles are commonly equipped with two suspension sets that work with different frequencies. The so called primary suspension is usually mounted between the wheelsets and the bogie frame, and deal with low amplitude, high frequency excitation that come from the wheel-rail interface. The secondary suspension is assembled, more often than not, between bogie frame and carbody, has a much larger vertical travel, and filters lower frequencies. Both are important and tuned to match safety, performance, and comfort standards.

In this paper, we deal with a rather uncommon secondary suspension arrangement that is used on the Vale operated railways Carajás (EFC) and Vitóra to Minas (EFVM). In these, the bogies are based on the French Y32 model, but equipped with a set of coil and tall rubber springs, while the usual suspension would use either coil springs, air springs, or a combination of coil and air springs.

The rubber spring presents some modelling challenges. First of all, because of bulk size of the rubber element, not only the vertical stiffness, but also lateral and rotation stiffnesses are relevant. A second complication comes from the hyperelastic material that compose the element. Danko *et al.* (2022), for instance, present some results for a finite element model developed for an automotive bushing using the well known Yeoh equations for hyperelastic constitutive behavior which coefficients were adjusted using experimental data. Their results showed that despite experimental curves for the test specimens were known, the dynamic stiffness for the tested and simulated bushing was significantly different for a wide range of frequencies. Berg (1997) presented a first model for the dynamic description of a unidimensional rubber

spring, but more sophisticated models for rubber components used on railway vehicles was considered as a future need according to Bruni *et al.* (2011) and few works addressed this topic since then: Alonso *et al.* (2013) developed a railroad rubber bushing model using fractional derivatives; Spiroiu (2018) presented a study on air springs assemble with parallel rubber cushions, but using only the vertical stiffness of such elements; Luo *et al.* (2016) analyzed the stress softening effect of rubber on a layered railroad spring, but did not address dynamical effects.

Using a procedure analogous to the one presented by Lima *et al.* (2022), in this work we use a concise set of experimental data to calibrate a finite element model of a tall rubber spring assembled in parallel to a coil steel spring used in the secondary suspension of the passenger coaches the run on the Vitória a Minas and Carajás railroads in Brazil. Piecewise linear curves of force-displacement that describe behavior are extracted from the finite element model and fed into a multibody model of the rail coaches. The dynamic behavior in terms of derailment coefficient (Nadal's coefficient, or L/V) and the the wear number ($T\gamma$) was analyzed, and compared to a baseline model that was developed using a unidirectional, linear suspension spring.

2. MODELS AND METHODOLOGY

To study the effect of the non-linearity of the secondary suspension's stiffness on safety and wheel wear, it was first necessary to estimate the non-linearity in the elastic behavior of the spring set formed by the coil spring and the rubber spring. This non-linear behavior was characterized by comparing Finite Element Analysis (FEA) with experimental data. Once the elastic behavior had been determined, multibody dynamics simulations were made to compare the Nadal coefficient and wear number. The Y32 bogie utilized in the simulations used two different secondary suspension configurations: non-linear stiffness and linear stiffness. Three tracks were chosen to carry out this analysis. Two of the tracks represent common curves experienced in the operation of these vehicles, while the third track represents the twisted track curve defined by European norm EN 14363:2019.

2.1 Multibody Dynamics Model of Y32 Bogie

The multibody model of the passenger car bogie adapted in this work was modeled using SIMPACK software. The bogie model was divided into seven rigid bodies, as shown in Figure 1. The kinematic links connecting the trailing-arm to the frame structure were modeled with spring and damping elements in parallel, with the center-pivot and bolster fixed to the carbody. Pitch revolution joints were used to connect the anti-roll bar links to the frame structure and to connect the trailing-arms to the wheelsets. The Watt block is linked to the center-pivot with a revolution joint in yaw.

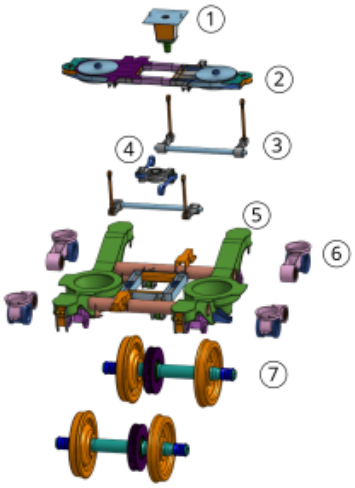

1. Center-pivot.
2. Bolster.
3. Anti-roll bar.
4. Watt block.
5. Frame.
6. Trailing-arm.
7. Wheelset.

Figure 1: Rigid bodies of the Y32 bogie used in multibody dynamics simulations.

2.2 Suspension Description

The primary suspension is formed by coil springs and linear dampers at each of the four wheelset bearings that connect to the frame. The primary suspension coil springs are composed of two springs in parallel, one inside the other. The secondary suspension of the Y32 bogie is composed of two vertical non-linear dampers, one lateral non-linear damper, two anti-roll bars, and two sets of springs formed by a coil spring and two rubber springs positioned inside the coil springs. The two rubber springs are aligned by a guide plate positioned between the rubber springs. Figure 2a shows the primary and secondary suspension elements described above and Figure 2b shows the set of springs of in the secondary

suspension.

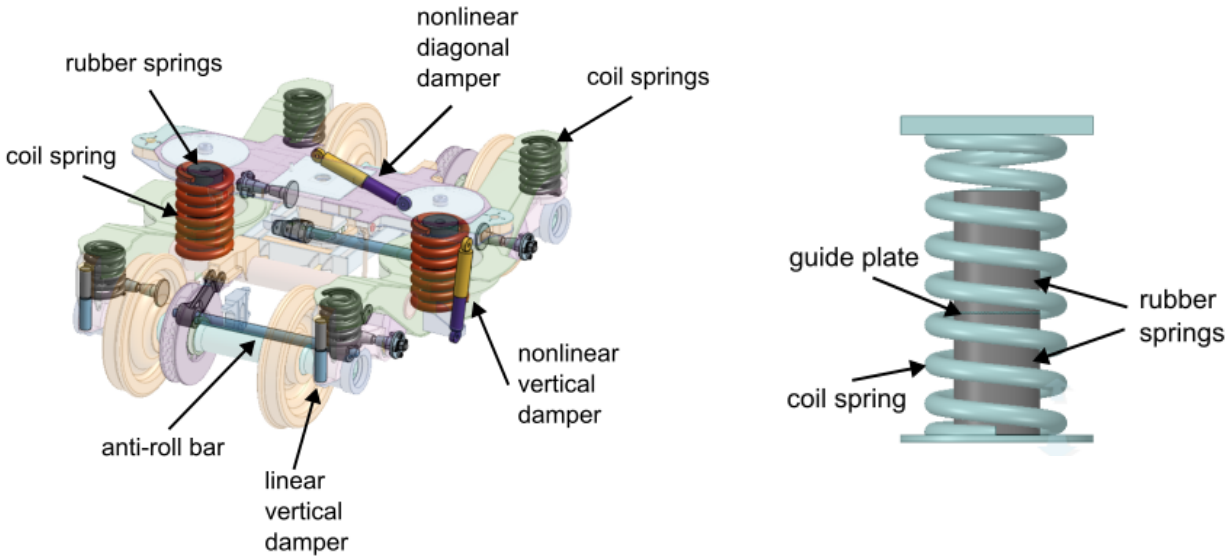

(a) (b)

Figure 2: Components suspension of Y32 bogie (a) and secondary suspension's spring pack (b)

2.3 Material Models Used in Finite Element Method

The coil spring material was modeled in FEA as linear elastic with $E = 207\,\text{GPa}$, $\nu = 0.3$. The rubber springs were modeled as Mooney-Rivlin hyperelastic materials with constants $C01 = 0.1\,\text{MPa}$, $C10 = 0.6\,\text{MPa}$ and $D01 = 0.00158MPa$. The rubber spring constants were determined through data obtained from a compression test on a spring test machine.

2.4 Axial non-linear Stiffness Model

To determine the force-displacement curve of the secondary suspension's spring sets, a static analysis using ANSYS Workbench software was performed in the axial direction, as shown in Figure 3. The implemented boundary conditions were:

- Fixed support on the lower base;
- Vertical symmetry;
- Prescribed displacement applied to the upper base in the direction of compression.

In addition to these boundary conditions, a coefficient of friction of 0.8 was used for the contacting interfaces between the steel and rubber materials.

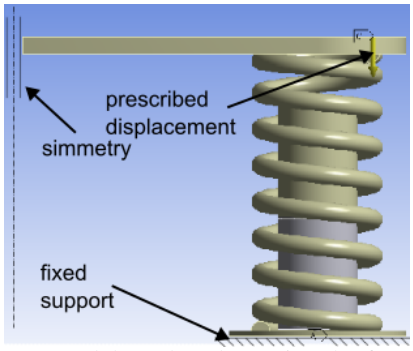

Figure 3: Configuration of the finite element model used to determine the force-displacement behavior of the spring set of the secondary suspension of the Y32 bogie in the axial direction.

Table 1: Set of prescribed displacements and their corresponding reaction forces applied in FEM simulation.

Displacement (mm)	4.2	50.0	75.0	100.0	150.0	160.0	200.0	250.0
Force (kN)	1.1	13.6	20.4	27.2	42.7	53.9	71.7	105.0

2.5 Radial Nonlinear Stiffness Model

To determine the force-displacement curve of the secondary suspension's spring set from FEA in the radial direction, a force was added at the upper base in the radial direction (red force in Figure 4). In this analysis, three simulations were performed, each with a preload value in the axial direction (yellow force in Figure 4). The preload intensities were chosen to result in axial deformations within the operating range verified by multibody dynamics simulations using constant stiffness. Table 2 summarizes the set of preloads and radial forces applied in each load step for the studied system.

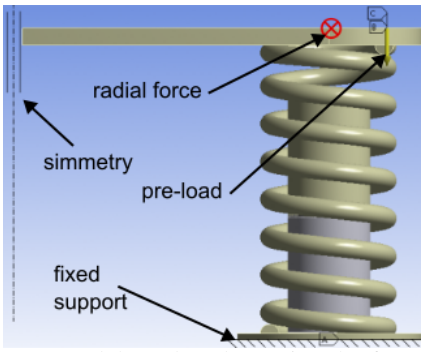

Figure 4: Configuration of the finite element model used to determine the force-displacement behavior of the spring set of the secondary suspension of the Y32 bogie in the radial direction.

Table 2: Set of prescribed displacements and their corresponding reaction forces applied in FEM simulation.

#	**Preload (kN)**	**Radial load (kN)**	**Radial load (kN)**	**Radial load (kN)**	**Radial load (kN)**	**Radial load (kN)**
1	48.2	1.0	5.0	10.0	15.0	20.0
2	71.8	1.0	5.0	10.0	15.0	20.0
3	91.0	1.0	5.0	10.0	15.0	20.0

2.6 Railway Tracks

Three tracks were used in the multibody dynamics simulations, with each track providing a different level of safety risk. All tracks are composed, in sequence, of a straight section, a clothoidal transition into the curve, the curve, a clothoidal transition out of the curve, and a straight section. Tracks 1 and 2 have conventional curve geometries, with the aim of providing results of the dynamic behavior of the vehicle under a less severe safety condition (Track 1) and a more severe safety condition (Track 2). Lastly, Curve 3 is based on DIN EN 14363:2019, and provides a critical situation in which the superelevation undergoes a sudden change while the vehicle is still navigating the central part of the curve. The relevant curve characteristics are shown in 3.

Table 3: Railway tracks descriptions

#	**Radius (m)**	**Length of curve (m)**	**cant (mm)**	**Transition (m)**	**Velocity (m/s)**
1	1119.0	202.0	17.9	10.4	15.3
2	134.0	120.0	63.5	30	8.89
3	150.0	200.0	26 $\rightarrow$ (-44)	30	2.78

3. RESULTS AND DISCUSSION

The results obtained in the analysis of the elastic behavior in the axial direction are shown in the graph of Figure 5a. It is possible to observe that the set of springs has a non-linear behavior that can be approximated by a piece-wise linear

model. The first linear region, with lower stiffness, corresponds to the application range in which the rubber spring is not required, while the second linear region describes the behavior of the springs acting together.

In the radial direction, the force-displacement results are shown in the graphs of Figure 5b. It can be observed that the curves obtained are non linear and are different for each axial preload. However, as the differences between preloads are not accentuated, it is reasonable to make the approximation using a single piece-wise linear model formed by two consecutive lines. In this model, the first straight line with the highest stiffness (around 785 N/mm) acts up to a displacement of approximately 9 mm, while the predominant stiffness in the second straight line (around 336 N/mm) acts beyond this displacement.

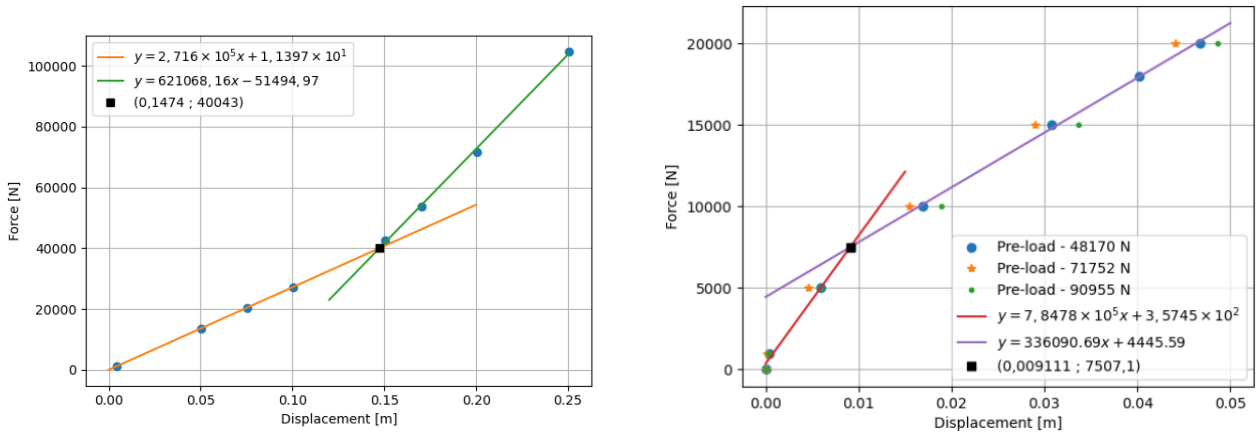

(a) (b)

Figure 5: Piecewise stiffnesses obtained from finite element analyses in (a) axial direction, and (b) radial direction.

The multibody simulations performed using the linear spring, and the spring presented in this paper are shown in Figures 6, 7, 8 with values for the Nadal coefficient, wear number on wheel thread, and wear number on the wheel flange respectively. Solid lines represent the results achieved using the piecewise stiffness model, while the dashed lines are the results for the constant stiffness spring. This constant stiffness is considered the same as the higher displacement curve from Figure 5.

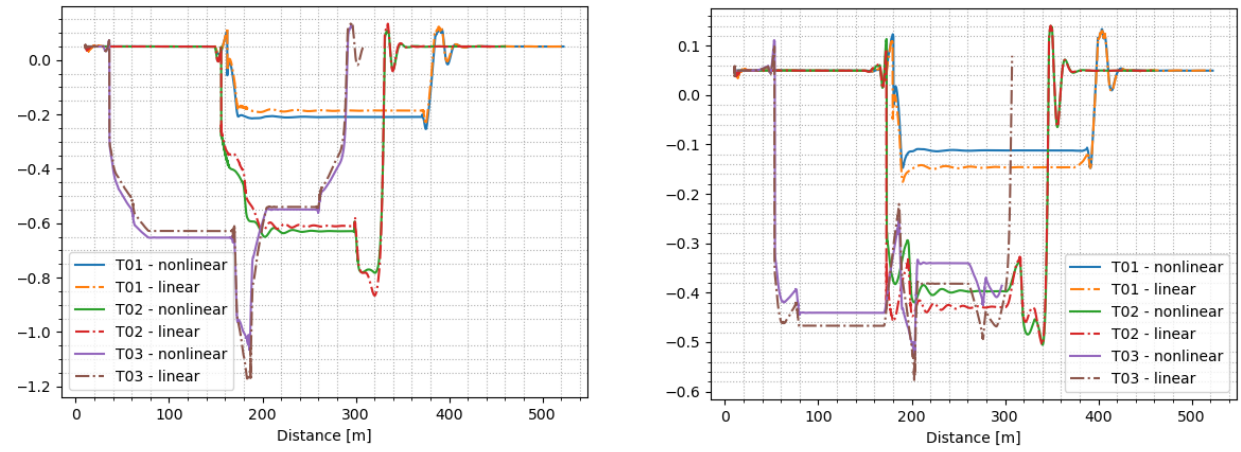

(a) (b)

Figure 6: Nadal's ratio of (a) left wheel from the front wheelset and front bogie, and (b) right wheel from the rear wheelset and rear bogie

From the plots in Figure 6, Nadal coefficient behavior for tracks 1 and 2 were, as expected, low in straight segments. When the coach enters the spiral transition to the curved sector, there is a transitory oscillation of the derailment ratio, followed by a stable value with higher amplitude than that of the straight zone of the track. When leaving the curve, the outer wheel flange touches the rail, causing again a L/V damped oscillation that is soon followed by a decrease in amplitude, reaching again the values presented in straight line. It is important to notice that tracks 1 and 2 are similar to the ones found in operation and, therefore, the derailment coefficient values are low, peaking 0,8 for the fully linear spring.

If on the one hand curves 1 and 2 present small derailment tendency, on the other track 3 presents a severe cant inversion defect in order to induce rail climbing and derailment. Safety risks, therefore, are expected to be higher, as

Nadal values. This can be verified on the purple and brown curves in Figures 6a e 6b.

The absolute L/V values are clearly different when on compares the results obtained using the piecewise stiffness and the linear stiffness springs. The results for the outer wheel of the attack bogie obtained using the simple linear model presented L/V values $13\,\%$, $12\,\%$ and $10\,\%$ higher compared to the piecewise stiffness spring for tracks 1, 2, and 3 respectively. For the inner wheel of the trailing bogie, the differences read $13\,\%$, $2\,\%$ and $12\,\%$ higher for the simple linear spring.

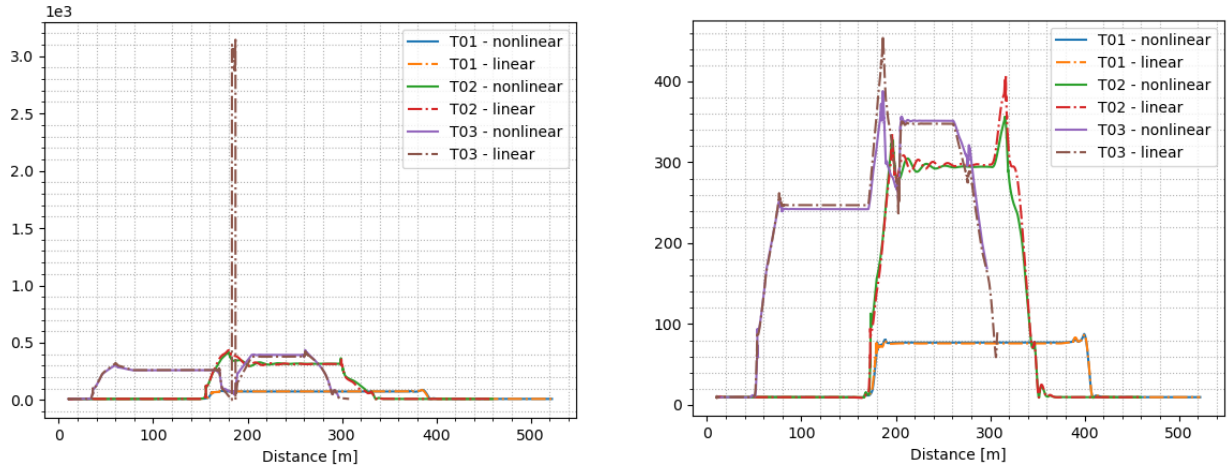

(a) (b)

Figure 7: Wear number in "pista" of (a) left wheel from the front wheelset and front bogie, and (b) left wheel from the front wheelset and rear bogie

Wear number plots, Figures 7, 8, also present the expected behavior: low values for tangent track spams, resulting from the almost pure rolling of the wheels, and higher values for the spiral and circular parts of the track, where lateral thread slip and flange contact are expected to happen due to inertia. Peak values occur when entering and leaving the curve, where flange impacts may occur.

For track 3, the sudden change in cant in the middle of the curve promotes, at first, a small drop in wear number, followed by a severe increase in thread contact $T\gamma$, as shown in Figure 7a. The initial reduction in wear number is mainly due to the fact that the outer wheels find a track that is lower than the previous sector. For the simple linear model, the wheel even loses contact with the rail for a small time, which is followed by an impact that translates into the peak observed in the position $185\,\mathrm{m}$ in Figure 7a(a). This impact phenomenon can also be noticed in Figure 8a, where it is shown that at $185\,\mathrm{m}$ there is a sudden drop of wear on the flange.

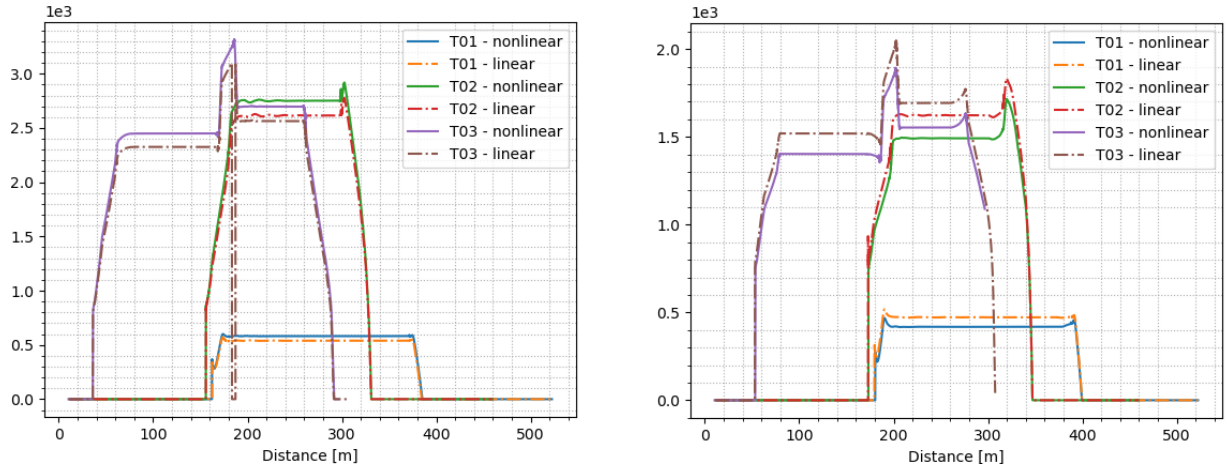

(a) (b)

Figure 8: Wear number in cant of (a) left wheel from the front wheelset and front bogie, and (b) left wheel from the front wheelset and rear bogie

It is noticeable in Figure 7a that the maximum $T\gamma$ for the outer wheel of the leading bogie front wheelset for tracks 1 and 2 did not change, in spite of the spring model adopted. For the outer wheel of the front wheelset of the trailing bogie, changin the spring model did not produce any considerable change in track 1, but results were affected for tracks 2 and 3,

resulting in changes of $15\,\%$ and $17\,\%$ respectively.

Wear number values for flange contact, conversely, changed for all tracks when different spring models were used. The outer front wheel of leading bogie faced differences of $6\,\%$ for track 1, $7\,\%$ for track 2, and $8\,\%$ for track 3. The differences for the front outer wheel of the trailing bogie reached $11\,\%$ for track 1, $7\,\%$ for track 2, and $8\,\%$ for track 3.

4. CONCLUSIONS

The influence of static stiffness non-linearity in secondary suspension rubber and coil springs of a passenger coach used in the Vitória a Minas and Carajás railroads was studied using force versus displacement curves in axial and radial directions derived from finite element simulations adjusted by a small set of experiments.

The results showed sensible differences to the baseline model, which was modelled using a simply linear stiffness curves. Those changes were noticed both in derailment coefficient, and in wear number. The data suggests that there is room for further improvement on the understanding of the exact behavior of the combination of steel coil and tall rubber springs, and that exact material characterization of the elastomeric part of these springs could help design and operation of the passenger coaches.

5. ACKNOWLEDGEMENTS

The authors would like to thank Vale S.A. for their monetary and informational contributions.

6. REFERENCES

Alonso, A., Gil-Negrete, N., Nieto, J. and Giménez, J., 2013. "Development of a rubber component model suitable for being implemented in railway dynamic simulation programs". *Journal of Sound and Vibration*, Vol. 332, No. 12, pp. 3032–3048. ISSN 0022460X. doi:10.1016/j.jsv.2013.01.002. URL https://linkinghub.elsevier.com/retrieve/pii/S0022460X13000047.

Berg, M., 1997. "A model for rubber springs in the dynamic analysis of rail vehicles". *Proceedings of the Institution of Mechanical Engineers, Part F: Journal of Rail and Rapid Transit*, Vol. 211, No. 2, pp. 95–108. ISSN 0954-4097, 2041-3017. doi:10.1243/0954409971530941. URL http://journals.sagepub.com/doi/10.1243/0954409971530941.

Bruni, S., Vinolas, J., Berg, M., Polach, O. and Stichel, S., 2011. "Modelling of suspension components in a rail vehicle dynamics context". *Vehicle System Dynamics*, Vol. 49, No. 7, pp. 1021–1072. ISSN 0042-3114, 1744-5159. doi:10.1080/00423114.2011.586430. URL http://www.tandfonline.com/doi/abs/10.1080/00423114.2011.586430.

Danko, J., Nemec, T., Milesich, T. and Magdolen, , 2022. "Dynamic Stiffness Determination of the Rubber Bushing Fem Modelwith Viscoelastic Material Behaviour". *Strojnícky časopis - Journal of Mechanical Engineering*, Vol. 72, No. 3, pp. 121–128. ISSN 2450-5471. doi:10.2478/scjme-2022-0046. URL https://www.sciendo.com/article/10.2478/scjme-2022-0046.

Eickhoff, B., Evans, J. and Minnis, A., 1995. "A Review of Modelling Methods for Railway Vehicle Suspension Components". *Vehicle System Dynamics*, Vol. 24, No. 6-7, pp. 469–496. ISSN 0042-3114, 1744-5159. doi: 10.1080/00423119508969105. URL http://www.tandfonline.com/doi/abs/10.1080/00423119508969105.

Lima, E.A., Baruffaldi, L.B., Manetti, J.L.d.B., Santos, Jr, A.A.d. and Martins, T., 2022. "Effect of truck shear pads on the dynamic behaviour of heavy haul railway cars". *Vehicle System Dynamics*, Vol. 60, No. 4. doi: https://doi.org/10.1080/00423114.2020.1858120.

Luo, R.K., Mortel, W.J., Wu, X. and Peng, L.M., 2016. "Evaluation of stress softening of the rubber suspension used on rail vehicles". *Proceedings of the Institution of Mechanical Engineers, Part F: Journal of Rail and Rapid Transit*, Vol. 230, No. 1, pp. 15–23. ISSN 0954-4097, 2041-3017. doi:10.1177/0954409714524748. URL http://journals.sagepub.com/doi/10.1177/0954409714524748.

Spiroiu, M.A., 2018. "Railway Vehicle Pneumatic Rubber Suspension Modelling and Analysis". *Mat.Plast.*, Vol. 55, No. 1, pp. 24–27. ISSN 0025-5289, 2668-8220. doi:10.37358/MP.18.1.4956. URL https://revmaterialeplastice.ro/Articles.asp?ID=4956.

7. RESPONSIBILITY NOTICE

The authors are solely responsible for the printed material included in this paper.